

## Catalytic Oxidation of Trichloroethylene over Pd-Loaded Sulfated Zirconia

Jung-Nam Park, Chul Wee Lee,\* Jong-San Chang,<sup>†</sup> Sang-Eon Park,<sup>‡,\*</sup> and Chae-Ho Shin<sup>§</sup>

*Advanced Chemical Technology Division, KRICT, P. O. Box 107, Yuseong, Daejeon 305-600, Korea*

*<sup>†</sup>Catalysis Center for Molecular Engineering, KRICT, P. O. Box 107, Yuseong, Daejeon 305-600, Korea*

*<sup>‡</sup>Department of Chemistry, Inha University, Incheon 402-751, Korea*

*<sup>§</sup>Department of Chemical Engineering, Chungbuk National University, Cheongju, Chungbuk 361-763, Korea*

*Received March 2, 2004*

The oxidative decomposition of trichloroethylene (TCE) was investigated using palladium catalysts supported on pure and sulfated zirconia. The reactions were performed under dry and wet conditions in the temperature between 200 and 550 °C keeping GHSV of 14,000 h<sup>-1</sup>. The products such as C<sub>2</sub>Cl<sub>4</sub>, C<sub>2</sub>HCl<sub>5</sub>, CO and CO<sub>2</sub> were observed in the reaction. The addition of water in the feed affected the distribution of reaction product with dramatically improved catalytic activity. The spectroscopic investigations gave an evidence that the strong acid sites play an important role on controlling the catalytic activity. Among the catalysts investigated, the Pd-loaded sulfated zirconia catalyst with 1 wt% Pd was found to exhibit the highest catalytic activity in the presence of water vapor having the stability for 30 h of the reaction at 500 °C. The successful performance of the catalyst might be attributed to promotional effect of Pd active sites and strong acid sites induced from surface sulfate species on zirconia.

**Key Words :** Trichloroethylene, Catalytic oxidation, Palladium, Sulfated zirconia

### Introduction

In view of the potential for the technological and economic advantage compared to the thermal incineration, catalytic oxidation of chlorinated volatile organic compounds (CVOC) has attracted attention as an efficient method for their destruction.<sup>1</sup> It is already known that thermal destruction of CVOC requires operating temperatures higher than 800 °C and in the process it produces highly toxic byproducts such as dioxine, dibenzofuran, nitrogen oxides etc. Among the CVOCs, TCE is mainly used in dry cleaning and degreasing processes as it is known to be hazardous to the environment and public health. As during the thermal incineration of TCE, substantial amounts of by-products such as carbon tetrachloride, tetrachloroethylene, hexachloroethane and hexachlorobutadiene were detected,<sup>2</sup> catalytic oxidation of TCE has been attempted for the complete removal of TCE to produce CO<sub>2</sub>, H<sub>2</sub>O and HCl at lower temperature.<sup>3-7</sup>

Sulfated metal oxides including sulfated zirconia have received great interests because of their high performances as solid superacid catalysts.<sup>8-10</sup> However, less attention has been paid to their capability as a catalyst for CVOC oxidation.<sup>11,12</sup>

The scope of this work is the preparation of Pd/SO<sub>4</sub>-ZrO<sub>2</sub> catalysts by impregnation with different Pd concentrations, the characterization of their properties, and the evaluation of their catalytic activities for TCE oxidation in the presence and absence of water vapor. The relationship between spectroscopic results and catalytic properties is also discussed. It is found that the surface sulfates provide the

strong adsorption sites for TCE while the Pd sites oxidize it effectively. This dual function leads to improved catalytic oxidation activity.

### Experimental Section

**Catalyst preparation.** Trichloroethylene (TCE) with 99% purity was purchased from Aldrich Co. Various palladium catalysts supported on zirconia (Pd/ZrO<sub>2</sub>) and sulfated zirconia (Pd/SO<sub>4</sub>-ZrO<sub>2</sub>) with different Pd loadings were prepared by impregnation with aqueous ammonia solution of PdCl<sub>2</sub> onto SO<sub>4</sub>-ZrO<sub>2</sub> and ZrO<sub>2</sub>, followed by drying at 100 °C and calcination at 550 °C for 5 h. Typically, in order to prepare 1.0 wt% Pd catalyst supported on SO<sub>4</sub>-ZrO<sub>2</sub>, simply being designated hereinafter as Pd(1.0)/SO<sub>4</sub>-ZrO<sub>2</sub>, 0.0877 g of PdCl<sub>2</sub> was dissolved in 500 mL of 16% NH<sub>4</sub>OH into which 5 g of SO<sub>4</sub>-ZrO<sub>2</sub> was dispersed. ZrO<sub>2</sub> was prepared by calcining Zr(OH)<sub>4</sub> (MEL) at 550 °C in air<sup>13</sup> and SO<sub>4</sub>-ZrO<sub>2</sub> (MEL) was used as received from MEL company.

**Catalyst characterization.** X-ray powder diffraction (XRD) patterns were recorded on a Rigaku D/MAX-IIIB X-ray diffractometer with Cu K<sub>α</sub> radiation. X-ray photoelectron spectroscopy (XPS) measurements were performed at room temperature on a VG ESCALAB 210 spectrometer, with Al K<sub>α</sub> radiation generated at 300 watts. The analyses were operated at a pass energy of 20 eV and a step size of 0.1 eV. The acid strengths of the catalysts were determined by NH<sub>3</sub> temperature programmed desorption (TPD) using home-made apparatus. An NH<sub>3</sub>-TPD experiment was performed as follows. 20 mg samples were pretreated in a quartz reactor in a N<sub>2</sub> flow (20 mL/min) at 500 °C for 2 h. NH<sub>3</sub> adsorption was initiated after the sample was cooled to 100 °C in a 20 mL/min N<sub>2</sub> flow. NH<sub>3</sub> adsorption was performed at 100 °C

\*To whom the correspondence should be addressed. C. W. Lee (chulwee@kriict.re.kr), S.-E. Park (separk@inha.ac.kr)

up to saturation. To remove physically adsorbed  $\text{NH}_3$  from the surface, sample was exposed to a flow of  $\text{N}_2$  (40 mL/min) at 100 °C for 1 hr. Finally, the desorption was carried out from 100 to 600 °C at a heating rate of 10 °C/min in He flow. The adsorption and desorption of TCE was studied by FT-IR spectroscopy (Nicolet MAGNA-IR 560 Spectrometer) from room temperature to 300 °C. For the FT-IR experiments, a self-supported wafer of the catalyst was made and further pretreated in a vacuum of  $10^{-4}$  Torr at 450 °C for the overnight to clean the surface of a catalyst.

**Catalytic activity measurement.** Catalytic oxidation reactions were carried out under atmospheric pressure in a fixed bed quartz reactor. Reaction conditions were GHSV = 14,000  $\text{h}^{-1}$ , [TCE] = 1000 ppm and [ $\text{H}_2\text{O}$ ] = 10,000 ppm. Air was used for the balance to maintain a constant gas flow. The effluents from the reactor were analyzed on-line by a Donam gas chromatograph equipped with a helium ionization detector (HID) and a BP-624 capillary column. The by-products such as tetrachloroethylene (PCE) were also identified and determined by the above GC after being separated in a GC column. Conversion of TCE was calculated by measuring the concentration of TCE before and after reaction. Concentrations of  $\text{CO}_2$  were determined by using Guardian  $\text{CO}_2$  analyzer.

## Results and Discussion

**Catalytic oxidation of trichloroethylene.** Table 1 illustrates the catalytic activities of various Pd-loaded  $\text{ZrO}_2$  and  $\text{SO}_4\text{-ZrO}_2$  at 50% and 90% conversion for the catalytic oxidation of TCE in the presence and absence of water vapor. The catalytic results indicate that the  $\text{SO}_4\text{-ZrO}_2$  support rather than  $\text{ZrO}_2$  support is able to show better performance for oxidative removal of TCE. In the absence of water vapor, it is observed that the conversion of TCE is improved by loading of Pd onto  $\text{SO}_4\text{-ZrO}_2$ . However, it is noted that the oxidation temperature in the presence of 10,000 ppm water vapor during the reaction decreases by 30–80 °C as compared with that of the absence of water vapor, indicating the weak interaction of water with surface active sites. This result is in contrast with the previous report that

the inhibitive effect by water vapor was observed over Pt/ $\gamma\text{-Al}_2\text{O}_3$  in TCE oxidation.<sup>14</sup> On the other hand, in the presence of water vapor, G.M. Bickle *et al.* reported that TCE destruction over Pt(0.9)/ $\text{ZrO}_2$  with greater than 99.9% conversion was achieved at 500 °C over a 100 h trial period in the condition of 13,000 ppm TCE, GHSV=5,000  $\text{h}^{-1}$ . It means that the use of  $\text{ZrO}_2$  as support is more effective in the presence of water vapor than that of  $\gamma\text{-Al}_2\text{O}_3$ .

It is evident that the use of  $\text{SO}_4\text{-ZrO}_2$  as catalyst support is advantageous, for example, Pd(1.0)/ $\text{SO}_4\text{-ZrO}_2$  can oxidize TCE more effectively than Pd(1.0)/ $\text{ZrO}_2$  at lower temperature by 85 °C in the presence of water vapor at  $T_{50}$ . This indicates that inclusion of Pd and  $\text{SO}_4$  into  $\text{ZrO}_2$  is effective for the decomposition of TCE. Among the catalysts investigated, the Pd(1.0)/ $\text{SO}_4\text{-ZrO}_2$  catalyst appears to be optimal for oxidative decomposition of TCE. The  $\text{SO}_4\text{-ZrO}_2$  catalyst has similar activity to those of Pd(0.5)/ $\text{SO}_4\text{-ZrO}_2$  and Pd(2.0)/ $\text{SO}_4\text{-ZrO}_2$ , indicating that  $\text{SO}_4\text{-ZrO}_2$  itself can oxidize TCE.

Since Pd(1.0)/ $\text{SO}_4\text{-ZrO}_2$  shows the highest catalytic activity for the oxidation of TCE, we have performed catalytic

**Table 1.** Catalytic oxidation of TCE in the absence and presence of water vapor<sup>d</sup>

Catalyst <sup>b</sup>	$T_{50}$ (°C) <sup>c</sup>		$T_{90}$ (°C) <sup>d</sup>	
	without $\text{H}_2\text{O}$	with $\text{H}_2\text{O}$	without $\text{H}_2\text{O}$	with $\text{H}_2\text{O}$
$\text{SO}_4\text{-ZrO}_2$	480	410	575	570
Pd(1.0)/ $\text{ZrO}_2$	410	385	515	465
Pd(0.5)/ $\text{SO}_4\text{-ZrO}_2$	450	370	550	525
Pd(1.0)/ $\text{SO}_4\text{-ZrO}_2$	330	300	510	465
Pd(1.5)/ $\text{SO}_4\text{-ZrO}_2$	385	330	530	470
Pd(2.0)/ $\text{SO}_4\text{-ZrO}_2$	450	400	510	525

<sup>a</sup>Reaction conditions: GHSV = 14,000  $\text{h}^{-1}$ ,  $\text{H}_2\text{O}$  = 10,000ppm. <sup>b</sup>Numbers in parenthesis means Pd loading in weight %. <sup>c</sup> $T_{50}$ : Temperature of 50% conversion. <sup>d</sup> $T_{90}$ : Temperature of 90% conversion.

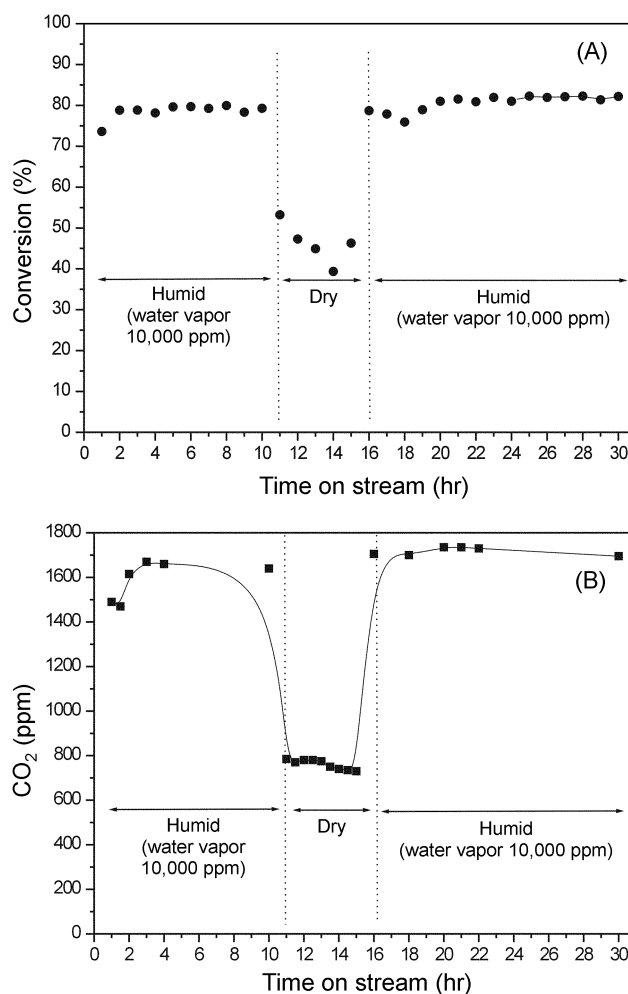


**Figure 1.** Effect of water vapor addition for the TCE conversion and  $\text{CO}_2$  formation over Pd(1.0)/ $\text{SO}_4\text{-ZrO}_2$  catalyst at 500 °C. Reaction conditions: TCE = 1,000 ppm,  $\text{H}_2\text{O}$  = 10,000 ppm, GHSV = 20,000  $\text{h}^{-1}$ .

oxidation of TCE for 30 h at 500 °C. Figure 1 shows TCE conversion over Pd(1.0)/SO<sub>4</sub>-ZrO<sub>2</sub>, and concentrations of CO<sub>2</sub> and CO formed during the oxidation of TCE. From this result, it is confirmed that Pd(1.0)/SO<sub>4</sub>-ZrO<sub>2</sub> is stable for 30 h and have the promotional effect in the presence of water vapor. As illustrated in Figure 1(A), 80% conversion is observed in the presence of water vapor, while, in a dry condition, the conversion is decreased to 50%. When water vapor is added again, conversion is recovered into its initial value without any decay. This behavior is also confirmed by the concentration of CO<sub>2</sub> produced, as shown in Figure 1(B). On the reintroduction of the water vapor, the concentration of CO<sub>2</sub> has been found to be recovered into its initial value without catalyst deactivation. While 7-12 ppm CO is produced in a dry condition (not shown), no CO is observed in a wet condition. This indicates that water vapor is attributed to the deep oxidation over the Pd/SO<sub>4</sub>-ZrO<sub>2</sub> catalysts.

**Characterization of catalysts.** The XRD patterns of ZrO<sub>2</sub>, Pd(1.0)/ZrO<sub>2</sub>, SO<sub>4</sub>-ZrO<sub>2</sub> and Pd(1.0)/SO<sub>4</sub>-ZrO<sub>2</sub> are given in Figure 1. ZrO<sub>2</sub> and Pd(1.0)/ZrO<sub>2</sub> possess the monoclinic zirconia phase, whereas SO<sub>4</sub>-ZrO<sub>2</sub> and Pd(1.0)/SO<sub>4</sub>-ZrO<sub>2</sub> have the tetragonal phase with no significant change in XRD pattern. It is interesting to note that the XRD intensities of Pd-loaded ZrO<sub>2</sub> and SO<sub>4</sub>-ZrO<sub>2</sub> are stronger than those of ZrO<sub>2</sub> and SO<sub>4</sub>-ZrO<sub>2</sub>, indicating that Pd(1.0)/ZrO<sub>2</sub> and Pd(1.0)/SO<sub>4</sub>-ZrO<sub>2</sub> catalysts become more crystalline after Pd loading than their supporting carriers. The improvement of crystallinity of catalysts after Pd loading promoted the catalytic activities, compared with supports before Pd loading.

It has been proposed that the activity of the catalyst supported on SO<sub>4</sub>-ZrO<sub>2</sub> is correlated with the ratio of Brønsted to Lewis acid sites of the SO<sub>4</sub>-ZrO<sub>2</sub> support.<sup>15</sup> It has been reported that the infrared spectra of pyridine cannot be used for the determination of the superacid character of SO<sub>4</sub>-ZrO<sub>2</sub>.<sup>16</sup> Therefore, NH<sub>3</sub>-TPD was used to characterize the nature and strength of the acid sites on SO<sub>4</sub>-ZrO<sub>2</sub> and Pd-

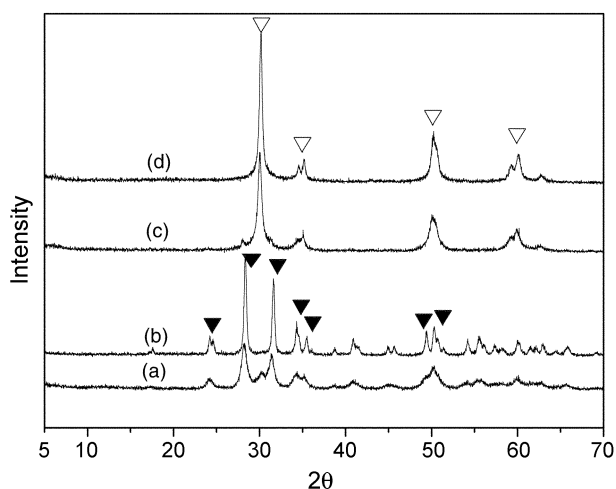


**Figure 2.** XRD patterns of (a) ZrO<sub>2</sub>, (b) Pd(1.0)/ZrO<sub>2</sub>, (c) SO<sub>4</sub>-ZrO<sub>2</sub>, and (d) Pd(1.0)/SO<sub>4</sub>-ZrO<sub>2</sub> catalysts, where ▼ and ▽ indicate monoclinic phase and tetragonal phase, respectively.

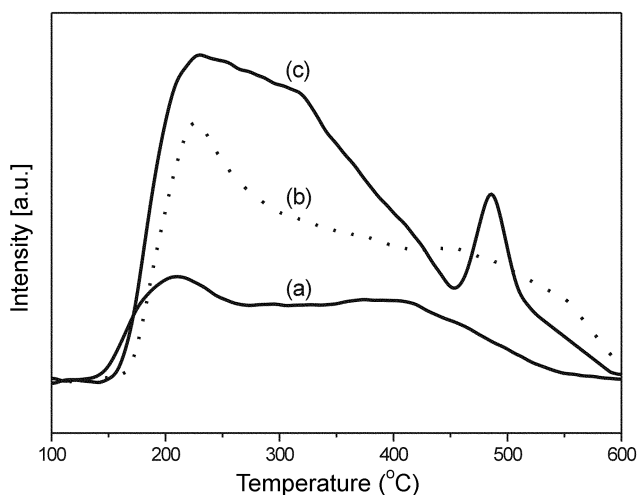


**Figure 3.** NH<sub>3</sub>-TPD profiles of (a) SO<sub>4</sub>-ZrO<sub>2</sub>, (b) Pd(1.0)/ZrO<sub>2</sub>, and (c) Pd(1.0)/SO<sub>4</sub>-ZrO<sub>2</sub> catalysts.

containing samples. As shown in Figure 3 for SO<sub>4</sub>-ZrO<sub>2</sub>, mainly three desorptions can be differentiated with the help of three broad peaks centered at 200, 300 and 400 °C. After loading Pd onto SO<sub>4</sub>-ZrO<sub>2</sub> the concentration of acid sites was increased by more than two times. Four different desorption peaks at 230, 330, 430 and 520 °C were observed. These peaks can be assigned to acid sites having low (230 °C) and medium-strong (330, 430 °C) range, similar to those as observed in the Y-type zeolite.<sup>17</sup> Remarkable observation in the NH<sub>3</sub>-TPD is the appearance of the narrow desorption peak at 520 °C which corresponds to a superacid site present on Pd(1.0)/SO<sub>4</sub>-ZrO<sub>2</sub>. Davis *et al.* observed a similar behavior and using XPS, attributed this behavior to a loss of water and/or an increase in surface concentration of sulfate with increasing time of activation at 500 °C.<sup>18</sup> It seems that the surface concentration of sulfate is increased by calcination after impregnation of Pd/SO<sub>4</sub>-ZrO<sub>2</sub> at 550 °C.

Figure 4(A) shows XP spectra of Pd(3d) and Zr(3p) for ZrO<sub>2</sub>, Pd(1.0)/ZrO<sub>2</sub>, SO<sub>4</sub>-ZrO<sub>2</sub> and Pd(1.0)/SO<sub>4</sub>-ZrO<sub>2</sub>, respectively. Since the maximum peak position of Zr(3d) is almost same as that of Pd(3d), it is not possible to clearly differentiate the two peaks. However, Pd(3d) peaks centered at about 336 and 341 eV in Pd(1.0)/SO<sub>4</sub>-ZrO<sub>2</sub> have a higher binding energy than those of Pd(1.0)/ZrO<sub>2</sub>. This indicates that Pd is highly dispersed on sulfated zirconia than on pure zirconia. The interesting observation in the XPS is the detection of a doublet, as shown in Figure 4(B), for Pd(1.0)/SO<sub>4</sub>-ZrO<sub>2</sub>. While a single symmetric peak is observed in the O<sub>1s</sub> region at 530.6 eV for Pd/ZrO<sub>2</sub>, an asymmetric peak is clearly observed for SO<sub>4</sub>-ZrO<sub>2</sub> and Pd(1.0)/SO<sub>4</sub>-ZrO<sub>2</sub>, respectively. The O<sub>1s</sub> peak obtained for the SO<sub>4</sub>-ZrO<sub>2</sub> is asymmetric with a shoulder on the higher binding energy side of the peak. When the Pd(1.0)/SO<sub>4</sub>-ZrO<sub>2</sub> sample is exposed to air for 5 h at 550 °C the peak shape becomes more asymmetric and is fitted well by two peaks centered at 531 and 530.6 eV, respectively. It is observed that the binding energy of O<sub>1s</sub> peak of ZrO<sub>2</sub> is higher than that of SO<sub>4</sub>-ZrO<sub>2</sub> by 0.9 eV, which is due to the inductive effect of

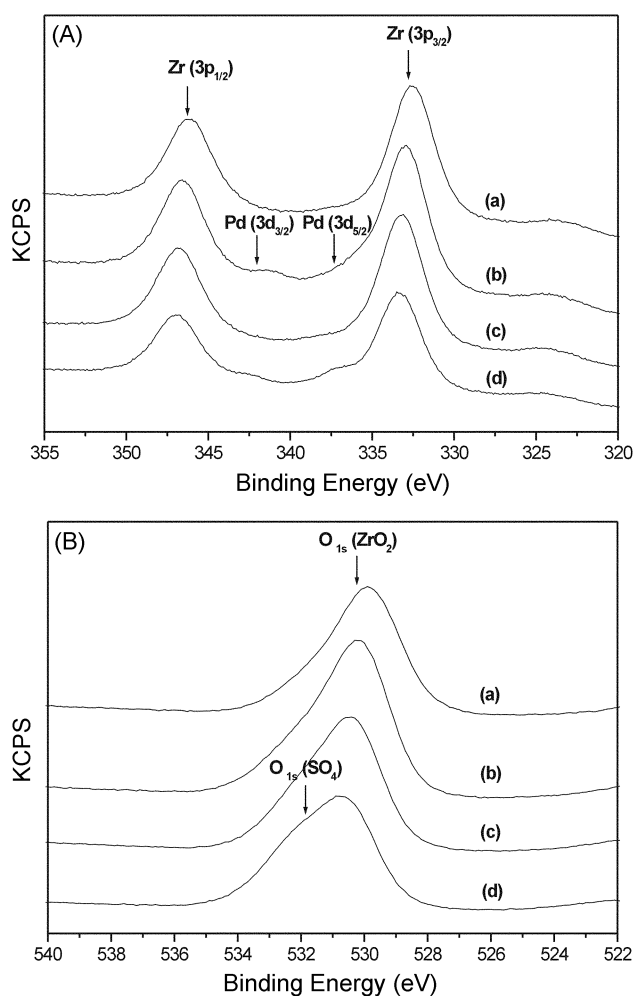


**Figure 4.** X-ray photoelectron (XP) spectra of (A)  $Zr_{3p}$  and  $Pd_{3d}$ , and (B)  $O_{1s}$  core levels on  $Pd(1.0)/ZrO_2$  and  $Pd(1.0)/SO_4-ZrO_2$  catalysts: (a)  $ZrO_2$ , (b)  $Pd(1.0)/ZrO_2$ , (c)  $SO_4-ZrO_2$  and  $Pd(1.0)/SO_4-ZrO_2$ .

the sulfate group. Similar results have been reported previously.<sup>18</sup> The higher binding energy  $O_{1s}$  peak agrees with the binding energy expected for oxygen in a sulfate group. This suggests that the  $SO_4$  present in the catalyst must be sufficiently close to the surface to be detected by XPS.

Figure 5 compares the adsorption/desorption of TCE over  $Pd(1.0)/ZrO_2$  and  $Pd(1.0)/SO_4-ZrO_2$ , respectively, monitored by FT-IR with different pre-treatments. For  $Pd(1.0)/ZrO_2$  (see Figure 5(A)), the self-supported pellet was initially pretreated *in vacuo* at 350 °C under vacuum. Upon adsorption of TCE at room temperature, bands are seen in the 1570–1630  $cm^{-1}$  which are associated with the  $-C=C-$  stretching vibrations and also bands of 931  $cm^{-1}$  and 835  $cm^{-1}$ , which are due to the C-Cl stretching, are observed. This indicates that TCE is molecularly adsorbed onto  $Pd(1.0)/ZrO_2$ .

When the sample was evacuated at room temperature, bands for  $-C=C-$  and  $-C-Cl$  disappear. After evacuation at 300 °C, intense bands at 1568 and 1445  $cm^{-1}$  are observed, which can be assigned to stretching vibrations of an acetate-type carboxylate group based on the literature data.<sup>19</sup> This

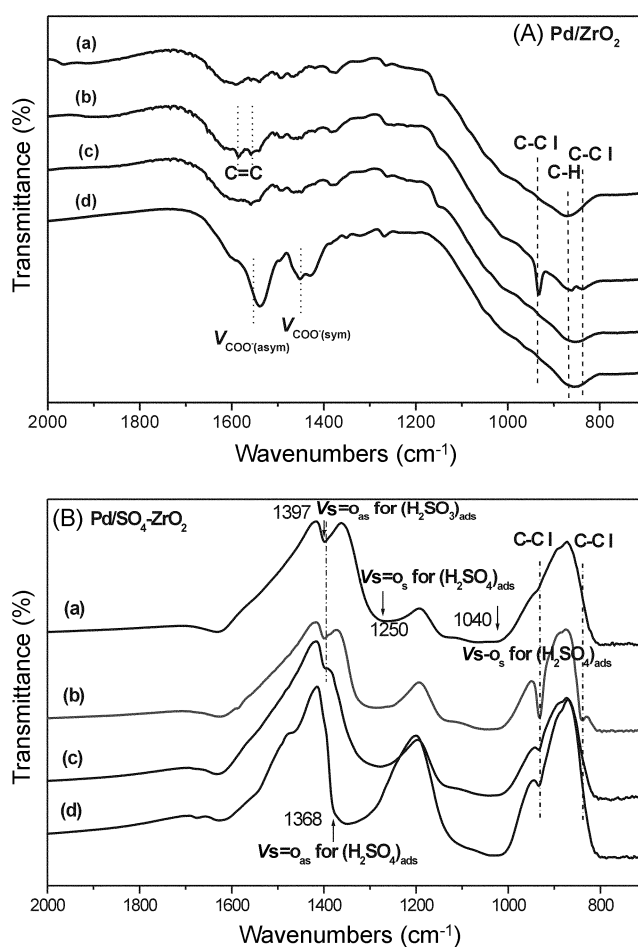


**Figure 5.** FT-IR spectra on adsorption/desorption of TCE over (A)  $Pd(1.0)/ZrO_2$  and (B)  $Pd(1.0)/SO_4-ZrO_2$  catalysts: (a) pretreatment at 350 °C for 5 hr, (b) adsorption 7 torr at RT, (c) desorption at room temperature by evacuation, and (d) desorption at 300 °C by evacuation.

observation can be proposed as the progressive catalytic oxidative decomposition of TCE. The adsorption/desorption of TCE over  $Pd(1.0)/SO_4-ZrO_2$  is different. For  $Pd(1.0)/SO_4-ZrO_2$  (see Figure 5(B)), pretreated at 350 °C, bands are observed at 1397, 1250 and 1040  $cm^{-1}$  which are assigned as  $(\nu_{s=O})_{asym}$  for adsorbed  $SO_3$  and  $(\nu_{s=O})_{sym}$  for adsorbed  $H_2SO_4$ , respectively. Upon adsorption of TCE at room temperature, intensity of the band at 1397  $cm^{-1}$  is reduced and new bands at 931 and 835  $cm^{-1}$  are immersed due to C-Cl stretching. The reduction in the intensity of the bands for C-Cl is clearly observed on evacuation at room temperature and 300 °C indicating that TCE is adsorbed over  $Pd(1.0)/SO_4-ZrO_2$  even at 300 °C under vacuum. It further indicates that superacid sites of  $SO_4-ZrO_2$  provides a strong adsorption site for TCE. When the sample was evacuated at 300 °C, only trace amount of the carboxylate group is observed in the range of 1570–1440  $cm^{-1}$ . This suggests that the decomposition pathway of TCE over  $Pd(1.0)/ZrO_2$  is different from that over  $Pd(1.0)/SO_4-ZrO_2$ .

It is not clear yet whether the peak intensity at 1397  $cm^{-1}$  grows upon evacuation of the sample at high temperature and overlaps with the peak of  $(\nu_{s=O})_{sym}$  at 1250  $cm^{-1}$ . It seems

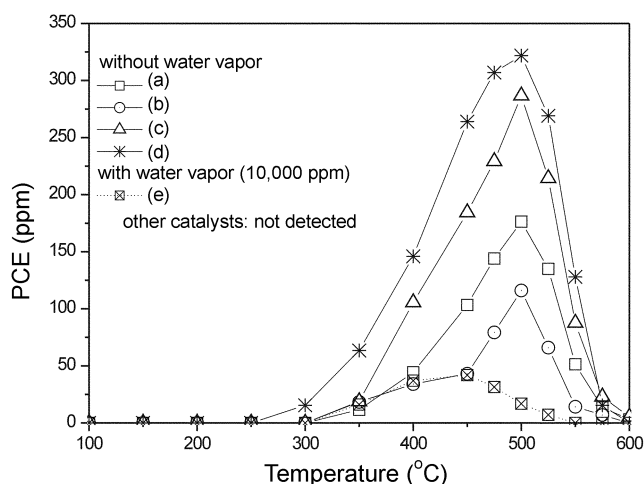


**Figure 6.** Concentrations of generated PCE as a function of temperature during the oxidation of TCE over various catalysts: (a) Pd(0.5)/SO<sub>4</sub>-ZrO<sub>2</sub>, (b) Pd(1.0)/SO<sub>4</sub>-ZrO<sub>2</sub>, (c) Pd(1.5)/SO<sub>4</sub>-ZrO<sub>2</sub>, (d) Pd(1.0)/ZrO<sub>2</sub>, (e) Pd(1.0)/ZrO<sub>2</sub>, other catalyst: not detected. Reaction conditions: TCE = 1,000 ppm, H<sub>2</sub>O = 10,000 ppm, GHSV = 14,000 h<sup>-1</sup>.

that, as suggested by Vedrin and co-workers,<sup>20</sup> sulfuric acid dehydrates upon evacuation at high temperature and forms the (SO<sub>3</sub>)<sub>ads</sub> species over ZrO<sub>2</sub>.

**The formation of by-products and reaction mechanism.** Since it is known that all chlorinated hydrocarbon produce substantial amount of HCl and Cl<sub>2</sub>, we did not attempt to determine them separately in the present study however, by-products such as chlorinated hydrocarbon, CO and CO<sub>2</sub> were determined.

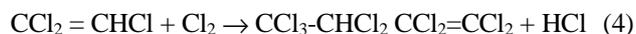
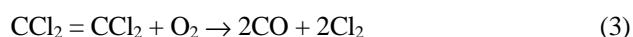
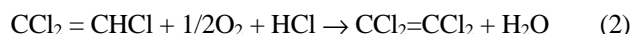
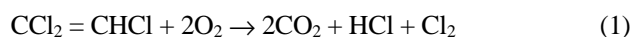
After oxidation of TCE, the main by-product is generated and identified as tetrachloroethylene (PCE). As shown in Figure 6, five different Pd-containing catalysts were tested for the formation of by-product as a function of the temperature during oxidation of TCE. In the presence of 10,000 ppm water vapor, only Pd(1.0)/ZrO<sub>2</sub> shows the formation of PCE less than 50 ppm at 450 °C, while no PCE is formed over the other four catalysts. In the absence of water, as expected, higher amount of PCE is generated. Over Pd(1.0)/ZrO<sub>2</sub>, the formation of PCE is started at 300 °C, and PCE is formed higher than 300 ppm at 500 °C, whereas over Pd(1.0)/SO<sub>4</sub>-ZrO<sub>2</sub>, the formation of PCE has started at 350 °C, PCE is formed about 120 ppm at 500 °C. In the case of Pd(0.5)/SO<sub>4</sub>-ZrO<sub>2</sub> and Pd(2.0)/SO<sub>4</sub>-ZrO<sub>2</sub>, about 170 ppm PCE is formed at 500 °C, while over Pd(1.5)/SO<sub>4</sub>-ZrO<sub>2</sub>, about 280 ppm PCE is formed at 500 °C.

In fact, over H-type zeolites and LaMnO<sub>3+δ</sub> perovskite catalyst, small amount of C<sub>2</sub>Cl<sub>4</sub> was detected even at the temperature higher than 500 °C under wet condition.<sup>14,21</sup> This implies that strong acid site or transition metal is not just good enough for the deep oxidation of chlorinated hydrocarbons. No C<sub>2</sub>Cl<sub>4</sub> is detected at 500 °C and wet condition, over Pd(1.0)/SO<sub>4</sub>-ZrO<sub>2</sub> bifunctional catalyst prepared in this study. Unknown by-product is also detected, in the absence of water vapor, 10 and 80 ppm of unknown by-product is generated at 500 °C over Pd(1.5)/SO<sub>4</sub>-ZrO<sub>2</sub>

and Pd(0.5)/SO<sub>4</sub>-ZrO<sub>2</sub> catalysts, respectively. This unknown by-product is expected as C<sub>2</sub>HCl<sub>5</sub> formed in the absence of water vapor during the oxidation of TCE.<sup>5,22</sup>

However, in the presence of water no unknown by-product is observed over Pd containing SO<sub>4</sub>-ZrO<sub>2</sub> catalysts. It means that formation of Cl<sub>2</sub> can be suppressed by the effect of water vapor represented as Deacon Reaction.

The possible reaction mechanism for TCE oxidation is suggested based on references as follows.<sup>18</sup> In the complete oxidation, TCE is converted to CO<sub>2</sub>, HCl and H<sub>2</sub>O. However, incomplete oxidation takes place with the generation of CO and some other byproducts such as PCE or C<sub>2</sub>HCl<sub>5</sub>. By-products such as PCE or C<sub>2</sub>HCl<sub>5</sub> formed during the TCE oxidation can be explained by chlorination followed by dehydrochlorination particularly in the absence of water vapor. Since TCE molecule contains more chlorine than hydrogen atom, Cl<sub>2</sub> would be formed easily in the absence of water vapor. By the introduction of water to the reaction mixture, an extra hydrogen source would be supplied for the HCl formation. Water can be used for the abatement of chlorine species from the catalyst surface so that the addition of water to the feed induces the reduction of formed Cl<sub>2</sub> by the reverse Deacon reaction.



## Conclusions

Several catalysts such as Pd/ZrO<sub>2</sub> and Pd/SO<sub>4</sub>-ZrO<sub>2</sub> have been prepared and compared their catalytic activities for TCE oxidation under dry and wet (10,000 ppm of water vapor) conditions. FT-IR, NH<sub>3</sub>-TPD and XPS demonstrates that acidity plays a significant role in the catalytic activity. The highly improved catalytic oxidation of TCE is observed over Pd(1.0)/SO<sub>4</sub>-ZrO<sub>2</sub>. This improvement might be due to the presence of Pd and strong acid site. The acid site (SO<sub>4</sub>) provides strong adsorption site for TCE while Pd can oxidize it easily, this is a kind of dual function of SO<sub>4</sub> and Pd for the enhancement of catalytic activity. The higher catalytic activity is also detected by the addition of water vapor into the reaction feed. The addition of water vapor has been proved to prevent the formation of toxic by-products such as PCE and C<sub>2</sub>HCl<sub>5</sub> in TCE oxidation implying deeper oxidation.

**Acknowledgement.** This work was supported by the Korean Energy Management Corporation and the Korean Ministry of Science and Technology for the Research Center for Nanocatalysis. This work was also supported by grant No. R01-2003-000-10069-0 from the Basic Research Program of the Korea Science & Engineering Foundation.

**References**

1. Josephson, J. *Environ. Sci. Technol.* **1984**, *18*, 222A.
  2. Yashuhare, A.; Morita, M. *Chemosphere* **1990**, *21*, 479.
  3. Kawi, S.; Te, M. *Catal. Today* **1998**, *44*, 101.
  4. Atwood, G. A.; Greene, H. L.; Chintawar, P.; Rachapudi, R.; Ramachandran, B.; Vogel, C. A. *Appl. Catal. B* **1998**, *18*, 51.
  5. González-Velasco, J. R.; Aranzabal, A.; Gutiérrez-Ortiz, J. I.; Lopez-Fonseca, R.; Gutiérrez-Ortiz, M. A. *Appl. Catal. B* **1998**, *19*, 189.
  6. Lopez-Fonseca, R.; Aranzabal, A.; Steltenpohl, P.; Gutiérrez-Ortiz, J. I.; González-Velasco, J. R. *Catal. Today* **2000**, *62*, 367.
  7. González-Velasco, J. R.; Lopez-Fonseca, R.; Aranzabal, A.; Gutiérrez-Ortiz, J. I.; Steltenpohl, P. *Appl. Catal. B* **2000**, *24*, 233.
  8. Davis, B. H.; Keogh, R. A.; Srinivasan, R. *Catal. Today* **1994**, *20*, 219.
  9. Corma, A.; Fornés, A.; Juan-Rajadell, M. I.; López Nieto, J. M. *Appl. Catal. A* **1994**, *116*, 151.
  10. Sohn, J. R.; Chun, E. W.; Pae, Y. I. *Bull. Korean Chem. Soc.* **2003**, *24*, 1785.
  11. Jiang, X.-Z.; Zhang, L.-Q.; Wu, X.-H.; Zheng, L. *Appl. Catal. B* **1996**, *9*, 229.
  12. Bickle, G. M.; Suzuki, T.; Mitara, Y. *Appl. Catal. B* **1994**, *4*, 141.
  13. Mekhemer, Gamal A. H. *Colloids and Surfaces A: Physico-chemical and Engineering Aspects* **1998**, *141*, 227.
  14. Lopez-Fonseca, R.; Aranzabal, A.; Gutiérrez-Ortiz, J. I.; Álvarez-Uriarte, J. I.; González-Velasco, J. R. *Appl. Catal. B* **2001**, *30*, 303.
  15. Nascimento, P.; Akatopoulou, C.; Oszagyan, M.; Coudurier, G.; Travers, C.; Joly, J. F.; Vedrin, J. C. *Stud. in Surf. Sci. & Catal.* **1993**, *75*, 1185.
  16. Corma, A.; Fornés, V.; Juan-Rajadell, M. I.; Lopez Nieto, J. M. *Appl. Catal. A* **1994**, *116*, 151.
  17. Wang, B.; Lee, C. W.; Cai, T.-X.; Park, S.-E. *Bull. Korean Chem. Soc.* **2001**, *22*, 1056.
  18. Milburn, D. R.; Keogh, R. A.; Srinivasan, R.; Davis, B. H. *Appl. Catal. A* **1996**, *147*, 109.
  19. Chintawar, P. S.; Green, H. L. *J. Catal.* **1997**, *165*, 12.
  20. Babou, F.; Coudurier, G.; Vedrin, J. C. *J. Catal.* **1995**, *152*, 341.
  21. Sinquin, G.; Petit, C.; Libs, S.; Hindermann, J. P.; Kiennemann, A. *Appl. Catal. B* **2001**, *32*, 37.
  22. Feijen-Jeurissen, M. M. R.; Jorna, J. J.; Nieuwenhuys, B. E.; Sinquin, G.; Petit, C.; Hindermann, J.-P.; *Catal. Today* **1999**, *54*, 65.
-